AIP | Review of Scientific Instruments

Internal magnetic field measurement on C-2 field-reversed configuration plasmas

H. Gota, M. C. Thompson, K. Knapp, A. D. Van Drie, B. H. Deng et al.

Citation: Rev. Sci. Instrum. **83**, 10D706 (2012); doi: 10.1063/1.4729497
View online: http://dx.doi.org/10.1063/1.4729497
View Table of Contents: http://rsi.aip.org/resource/1/RSINAK/v83/i10
Published by the American Institute of Physics.

Internal magnetic field measurement on C-2 field-reversed configuration plasmas[a)]

H. Gota,[b)] M. C. Thompson, K. Knapp, A. D. Van Drie, B. H. Deng, R. Mendoza, H. Y. Guo, and M. Tuszewski
Tri Alpha Energy, Inc., Rancho Santa Margarita, California 92688, USA

(Presented 9 May 2012; received 7 May 2012; accepted 25 May 2012; published online 28 June 2012)

A long-lived field-reversed configuration (FRC) plasma has been produced in the C-2 device by dynamically colliding and merging two oppositely directed, highly supersonic compact toroids (CTs). The reversed-field structure of the translated CTs and final merged-FRC state have been directly verified by probing the internal magnetic field structure using a multi-channel magnetic probe array near the midplane of the C-2 confinement chamber. Each of the two translated CTs exhibits significant toroidal fields (B_t) with opposite helicity, and a relatively large B_t remains inside the separatrix after merging. © *2012 American Institute of Physics*. [http://dx.doi.org/10.1063/1.4729497]

I. INTRODUCTION

A field-reversed configuration (FRC) is a high-β compact toroid (CT) which has predominantly poloidal magnetic field with zero or small self-generated toroidal magnetic field.[1,2] The FRCs have been produced by the field-reversed theta-pinch (FRTP) technique with or without translation along a geometrical axis. The translated FRC has been demonstrated to be robust in translation,[3] and the theta-pinch CT translation/merging technique has recently been further explored.[4–7]

A large θ-pinch/merging system, C-2, was built to form high flux ($\phi_p > 10$ mWb), high temperature ($T_{\text{total}} > 500$ eV) FRC plasmas using the CT collision-merging technique. The C-2 device, as illustrated in Fig. 1, consists of a central confinement region surrounded by two FRTP formation sources and two divertors. The C-2 confinement chamber is made of stainless steel, which serves as a flux conserver on the timescale of the experiment, and the formation tubes are made of quartz. A set of dc-magnets generates a quasi-static axial magnetic field, B_z, throughout the device.

Magnetic probes are widely used in measurements of current-carrying plasma, particularly the area inside the separatrix is of interest to investigate. However, internal magnetic probes are often too disturbing to a plasma configuration in the high temperature and high density regime. Therefore, the design and development of a robust and minimally disturbing probe is a requirement. In past FRC experiments, Slough and Miller developed miniature, robust, multi-dimensional hand-wound internal magnetic probe arrays, and demonstrated less perturbation to the plasma configuration and more reliable measurements with appropriate selection of plasma facing materials and overall probe size.[8,9] In spheromak research, Romero-Talamás have developed a three-dimentional magnetic probe array whose pickup coils are commercial chip inductors which have precise dimensions, excellent consistency, and ease of use.[10]

The internal magnetic probe arrays presented here are of two kinds: (a) Three-axis magnetic field measurement using commercial chip inductors, and (b) Two-axis hand-wound pickup coils with better spatial resolution and smaller overall probe size than those of probe (a). In this paper, the probe designs and characteristics are described in Sec. II, and the measured magnetic field profiles of C-2 FRC plasmas are presented in Sec. III, including a poloidal flux estimated from the $B_z(r)$ profile as well as inferred from a rigid rotor (RR) model.

II. INTERNAL MAGNETIC FIELD PROBE DESIGN AND ASSEMBLY

A. Three-axis chip-inductor array (1st generation)

Thirty chip-inductors (manufactured by Coilcraft Inc., model 1008CS-472XGLB) were used for the three-axis probe array with 10 radial positions. The nominal dimensions of the chip inductors are 2.9 mm × 2.7 mm × 2.0 mm, the effective area of the coil is about 1.65 cm^2. A set of 3 chip-inductors with perpendicular orientation towards each other for B_z, B_t, and B_r measurements was mounted inside slots of a Delrin plastic rod, as shown in Fig. 2(a). The spacing between sets of 3 chip-inductors is 5 cm; thus the effective probe length is 45 cm.

Figure 2(b) illustrates a whole assembly of the internal magnetic probe array, which was installed in the midplane of the C-2 confinement vessel. The housing of the probe assembly was a SS304 tube with an outer diameter (OD) of 0.25 in. and a nominal wall thickness of 0.005 in. The end of the stainless steel tube was plugged, and the other end was welded to a 1.33 in. conflat flange and attached to a hollow-linear-feedthrough actuator (Thermionics, model FLMH-275-50-12); the housing played the role of the vacuum boundary. The

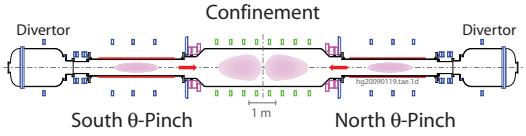

FIG. 1. Schematic of the C-2 device.

[a)]Contributed paper, published as part of the Proceedings of the 19th Topical Conference on High-Temperature Plasma Diagnostics, Monterey, California, May 2012.

[b)]Electronic mail: hgota@trialphaenergy.com.

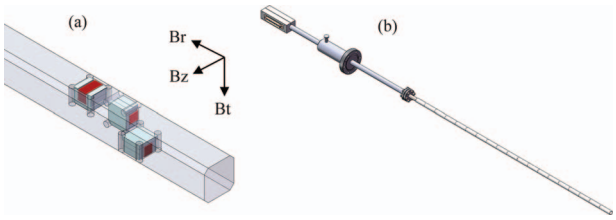

FIG. 2. Sketches of (a) the first set of three-axis chip-inductors with a Delrin rod and (b) the whole probe assembly installed on the C-2 midplane. Probe array coverage: $r = 0$–45 cm with a 5 cm spacing.

stainless steel tubing was fully covered by a thin wall teflon heat shrink tube in order to prevent an electrical interaction with the plasma, and on top of that boron-nitride (BN) jackets (Saint Gobain Advanced Ceramics, AX05 grade) were mounted as a plasma facing material. The BN piece was machined into interlocking tubes around 2 in. long and 7/16 in. OD. The first coil (B_z #1) reached the geometrical axis of the C-2 confinement vessel ($r = 0$), while the last one (B_z #10) was positioned at $r = 0.45$ m; here, the confinement vessel wall radius (r_w) is 0.7 m and a fixed regular B-dot probe was mounted near the chamber wall.[11] The 12-in. stroke actuator could move the probe position; e.g., for B_z #1, $r = 0$–30.5 cm.

B. Two-axis hand-wound coil array (2nd generation)

The two-dimensional internal magnetic field probe array consists of 16 hand-wound pickup loops in each of the z and θ directions (B_z and B_t), spaced 3 cm apart as shown in Fig. 3(a); i.e., the same effective probe length as the 1st generation probe array but with better spatial resolution. In order to make a small probe array, very fine but strong tungsten wire was selected and coils were wound by hand. The nominal size of the tungsten wire is ~1.5 mil, with gold plating for soldering purposes, and it is insulated by polyimide (Kapton) with a final OD of ~1.85 mil. The pickup loop has an effective area of ~3.4 cm^2 after 10 turns of winding, and the coil array was wrapped with a thin teflon tape to protect the fine wires. All twisted pairs of leads were connected to D-Sub 37-pin connectors, and the coil assembly was inserted into a newly fabricated 30-in. long hollow-linear-feedthrough actuator (Thermionics) and a 28-in. long end-capped SS304 tubing (Vita Needle Company) with ~0.165 in. OD and nominal 2 mil wall thickness.

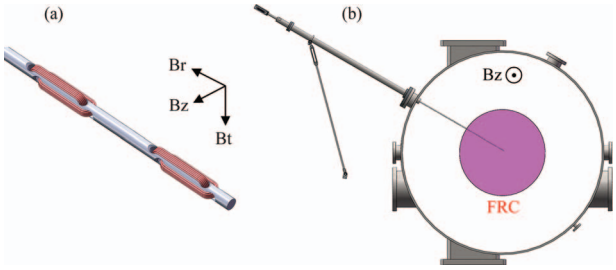

FIG. 3. (a) A sketch of the first pair of the two-axis hand-wound internal magnetic probe array, and (b) a cross-sectional view of the C-2 midplane with the probe assembly. Sixteen radial positions of B_z and B_t probe array cover $r = 0$–45 cm with a 3 cm spacing when the probe is fully inserted. The probe assembly can be fully retracted outside the vessel wall by the 30-in. long actuator.

The housing is the vacuum boundary, and a PEEK heat-shrink tubing (Zeus, Inc.) was used for the stainless steel tube insulation and surrounded by BN jackets, which have a quarter inch of OD and 35 mil thickness. With the long actuator and SS304 tubing, the probe array reaches the center of the confinement vessel ($r = 0$), as illustrated in Fig. 3(b), and also can be fully retracted outside the vessel wall when the titanium gettering system is in operational mode for vessel wall conditioning in order not to deposit titanium on the BN jacket.

C. Probe calibration and electronics

In both probe arrays, coils were individually calibrated using a Helmholtz coil with known field amplitude and direction. They were also calibrated *in situ* with the dc-field.

Initial internal B measurements were done with several signal integration techniques as well as different D-tacq cards; (i) a post-processing numerical integration with a 2 M samples/s D-tacq, (ii) a passive integration with RC time ~500 μs and the same D-tacq card, and (iii) an active integration with RC ~100 μs and a 500 kS/s D-tacq card. After several iterations of test and field measurements, the differential active integrators with the 2 MS/s D-tacq card were chosen for the 2nd generation of the probe array because of reliable system operation and ease of data handling, including dc-field correction.

III. EXPERIMENTAL RESULTS AND DISCUSSION

Both internal magnetic probe arrays were installed on the same port at the midplane of the C-2 confinement vessel, but each internal field measurement was conducted during different experimental campaigns.

First, the three-axis chip-inductor probe array was developed and installed in C-2. All 3 components of the magnetic field (B_z, B_t, and B_r) were successfully observed in both single-sided translated FRCs and collided-merging FRCs. Around the collision of two oppositely translated FRCs, in particular, very strong and complex field changes were detected; however, the B_r component was observed to quickly disappear after the collision, and it was difficult to extract more meaningful results due to the limitations of the measurement such as low signal level and low sampling rate. Figure 4 shows an example of B_z and B_t profiles during the relatively quiescent phase after the collision. As can be seen from the $B_z(r)$ profile, the field-reversed structure was directly verified although the internal probe degraded the FRC's performance, especially its lifetime.

Second, the upgraded internal magnetic probe array was built, as described in Sec. II B, and further experiments were conducted to investigate the dynamic changes of magnetic

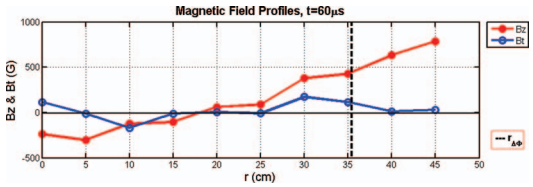

FIG. 4. Radial profiles of magnetic fields, $B_z(r)$ and $B_t(r)$, measured by the internal magnetic probe (three-axis chip-inductor array) mounted at the C-2 midplane. B_r was not measured in shot 12 211.

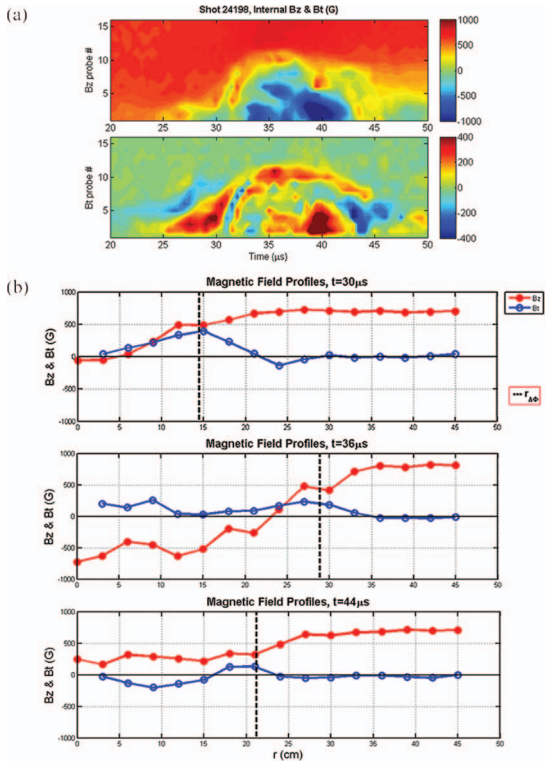

FIG. 5. (a) Contours of magnetic fields (B_z and B_t) as a function of time in the single-sided/translated FRC. Probe #1 corresponds to $r = 0$, and #16 locates at $r = 45$ cm with 3 cm spacing in between. (b) Time slices of magnetic field profiles at t = 30, 36, 44 μs.

fields in single-sided FRCs as well as collided-merging FRCs. The key of the upgrade was (i) smaller overall probe size with less perturbation to the FRC plasma, (ii) higher spatial probing resolution, especially inside the separatrix, and (iii) more data sampling to observe clear dynamic field changes.

Figure 5 shows a single-sided shot where the FRC was formed in the south-formation section and translated into the confinement vessel: (a) contours of $B_z(r)$ and $B_t(r)$ as a function of time; (b) time evolution of radial profiles of both B_z and B_t. As can be clearly seen in Fig. 5(a), very dynamic and strong toroidal fields were observed mainly inside the separatrix when FRC plasma passed by the internal probe array. Moreover, the sign of the toroidal magnetic field appeared to be opposite between the front and the rear of translated FRCs; this phenomenon was also identified in past translated FRC experiments.[3] Although the translated single-sided FRC did not live long due to its high translation speed and the presence of the internal magnetic probe array, the probe captured a nice field-reversed structure.

In the colliding FRC case, more violent and drastic changes of $B_z(r)$ and $B_t(r)$, particularly during the collision of two FRCs, have been observed, as shown in Fig. 6(a). The internal probe strongly degrades the FRC performance in terms of its configuration lifetime and radial displacement; however, the measured B_z profile appears to feature the field-reversed structure after merging, as seen in the example of Fig. 6(b). Each of the two translated FRCs exhibits significant toroidal fields with opposite helicity, and a relatively large B_t remains inside the separatrix after merging and throughout the FRC life.

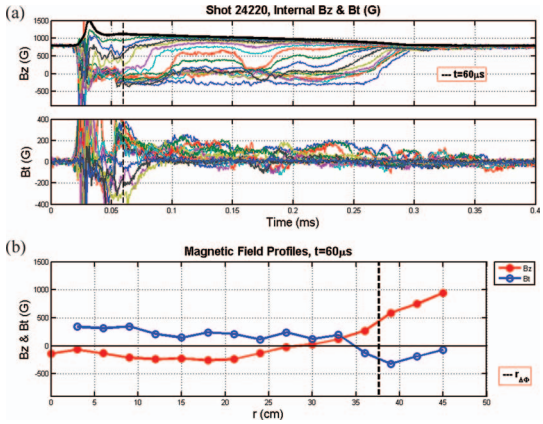

FIG. 6. (a) Time evolution of 16 sets of $B_z(r)$ and $B_t(r)$ during collided-merging FRCs shot, and (b) magnetic field profiles at t = 60 μs.

A RR model is a well-known and adequate profile model for the magnetic field and the density of FRCs.[1,2] The poloidal flux (ϕ_p) of the FRC can be approximately estimated from the excluded flux measurement with the RR model, expressed as follows:

$$\phi_{p\_\mathrm{RR}} \approx 0.31 x_s \Delta\Phi = 0.31\pi \frac{r_s^3}{r_w} B_e, \tag{1}$$

where x_s is the ratio of separatrix radius/vessel wall radius, $\Delta\Phi$ is the excluded flux, and B_e is the external field. By contrast, probing the magnetic field profile yields a relatively simple poloidal flux estimation by

$$\phi_p = -\int_0^R 2\pi r B_z dr = \int_R^{r_s} 2\pi r B_z dr, \tag{2}$$

where R is the field null radius. In the ideal case, the poloidal fluxes inside and outside of R are equal to each other. Based on the measurements (Fig. 6(b)), $\phi_{p\_\mathrm{in}} = 5.3$ mWb and $\phi_{p\_\mathrm{out}} = 4.1$ mWb as well as $\phi_{p\_\mathrm{RR}} = 8.3$ mWb were estimated. Poloidal fluxes inside and outside R are in close agreement, but the discrepancy in the estimated poloidal fluxes between direct measurement and RR model is possibly due to FRC position and structure.

ACKNOWLEDGMENTS

The authors would like to acknowledge the rest of the Tri Alpha Energy, Inc. staff for their system development support as well as useful discussions.

[1] M. Tuszewski, Nucl. Fusion **28**, 2033 (1988).
[2] L. C. Steinhauer, Phys. Plasmas **18**, 070501 (2011).
[3] H. Y. Guo, A. L. Hoffman *et al.*, Phys. Rev. Lett. **92**, 245001 (2004).
[4] G. Votroubek, J. Slough *et al.*, J. Fusion Energy **27**, 123 (2008).
[5] M. Binderbauer, H. Y. Guo *et al.*, Phys. Rev. Lett. **105**, 045003 (2010).
[6] H. Y. Guo, M. Binderbauer *et al.*, Phys. Plasmas **18**, 056110 (2011).
[7] M. Tuszewski, A. Smirnov *et al.*, Phys. Plasmas **19**, 056108 (2012).
[8] J. T. Slough and K. E. Miller, Rev. Sci. Instrum. **72**, 417 (2001).
[9] K. E. Miller, K. M. Velas *et al.*, "Miniature magnetic field probes for use in high temperature plasmas," Bull. Am. Phys. Soc. **54**, CP8.00014 (2009) (http://meetings.aps.org/link/BAPS.2009.DPP.CP8.14).
[10] C. A. Romero-Talamás, P. M. Bellan *et al.*, Rev. Sci. Instrum. **75**, 2664 (2004).
[11] M. C. Thompson, A. D. Van Drie *et al.*, "Magnetic diagnostic suite of the C-2 field-reversed configuration experiment confinement vessel," Rev. Sci. Instrum. (these proceedings).